Hindawi
Advances in Materials Science and Engineering
Volume 2022, Article ID 8366665, 11 pages
https://doi.org/10.1155/2022/8366665

Research Article

Acrylic Rubber-Reinforced Halloysite Nanotubes/Carbon Black Hybrid Fillers for Oil Seal Applications: Thermal Stability and Dynamic Mechanical Properties

K. Senthilvel,[1] **B. Prabu**,[2] **C. Moganapriya**,[3] **R. Rajasekar**,[4] **M. Francis Luther King**,[5] **and Md. Elias Uddin**[6]

[1]*Department of Mechanical Engineering, Karaikal Polytechnic College, Puducherry, Tamil Nadu, India*
[2]*Department of Mechanical Engineering, Puducherry Technological University, Puducherry, Tamil Nadu, India*
[3]*Department of Mining Engineering, Indian Institute of Technology Kharagpur, Kharagpur, West Bengal, India*
[4]*Department of Mechanical Engineering, Kongu Engineering College, Perundurai, Tamil Nadu, India*
[5]*Department of Mechanical Engineering, Swarnandhra College of Engineering and Technology, Narsapur, Andhra Pradesh, India*
[6]*Department of Leather Engineering, Faculty of Mechanical Engineering, Khulna University of Engineering and Technology, Khulna, Bangladesh*

Correspondence should be addressed to Md. Elias Uddin; eliasuddin@le.kuet.ac.bd

Received 29 June 2022; Revised 22 September 2022; Accepted 21 November 2022; Published 29 December 2022

Academic Editor: Georgios I. Giannopoulos

Copyright © 2022 K. Senthilvel et al. This is an open access article distributed under the Creative Commons Attribution License, which permits unrestricted use, distribution, and reproduction in any medium, provided the original work is properly cited.

In this study, we show that adding halloysite nanotubes (HNT) to carbon black (CB)-packed acrylic rubber (ACM) composites improves their thermal properties. The thermo-oxidative stability, thermal stability, and dynamic mechanical properties of ACM composites (filled simply with 70 phr CB) and ACM hybrid composites comprising a fixed amount of CB (60 phr) and a variable amount of halloysite nanotubes (HNT) (2, 4, 6, 8, and 10 phr) were investigated. As evidenced by the oxidation induction time analysis, hybrid structures support a higher degree of antioxidation in composites reinforced with twin fillers than composites reinforced just with CB. ACM composites with dual fillers had greater breakdown temperatures (temperatures at 10% weight loss (T_{10}) and 50% weight loss (T_{50})) and char residue concentration at 600°C than ACM conventional composites, according to thermogravimetric tests. The activation energy of the thermal disintegration of ACM composites, as determined by the Kissinger and Flynn–Wall–Ozawa techniques, shows that the addition of HNT improves the thermal stability of ACM composites. The storage modulus of ACM composites was increased by 79 percent at 30°C when 10 phr of black filler was replaced with 6 phr of tubular HNT, according to additional viscoelastic experiments.

1. Introduction

The last few decenniums have advocated a strong interest towards the development of high-performance polymeric materials with resistance to elevated or lower temperatures, flame retardation, and admissible mechanical properties. The most popular strategies for producing thermally stable materials are grafting polymeric backbones with polymers that demonstrate improved thermal stability, using high-temperature polymeric blends as the matrix, and dispersion of high-temperature-resistant filler particles. Fillers in the nanoscale range, to a greater or lesser extent less than 100 nm, have been actively explored in recent years in order to develop cutting-edge polymeric materials. Nanocomposites are made up of polymer and nanofiller combinations.

Polymer nanocomposites containing nanofiller in extremely small concentrations (1–8 phr) have been shown to have significantly greater thermal stability than standard materials in studies. Among the nanofillers, layered silicates have been a popular topic of study among scientists and businesses. Intercalation of organically modified layered

silicates, for example, has a considerable impact on the thermal stability of acrylonitrile butadiene nanocomposites [1]. The thermal stability of elastomeric nanocomposites with carbonaceous nanofiller, which includes various kinds of graphene and carbon nanotubes [2–7], has been studied in the literature in recent years. The enhancement in the thermal resistance of elastomers with the incorporation of nanofillers is largely due to the barrier effect. As contemplated by Vyazovkin et al. [8] and Gilman et al. [9], a polymeric-inorganic char builds upon the surface of the polymer and provides the mass and heat transfer barriers that augment the thermal resistance.

The thermal deterioration of elastomeric materials is a predominant issue, as it ultimately governs the mechanical attributes, durability, and service life of rubber components. As soon as the degradation commences, the above attributes will gradually deteriorate. Hence, understanding various thermal degradation parameters of elastomers is of paramount importance for developing a rational technology for elastomer processing and higher-temperature applications. The kinetic analysis of the thermal deterioration is very essential, as it can provide a breakthrough on the energy barriers of the process and offer clues for understanding degradation mechanisms. The challenge for studying thermal degradation kinetics is to find a reliable approach. Normally, the multiheating-rate method has been extensively used to study the thermal degradation kinetics due to its reliability. Several researchers have adopted the Kissinger and Flynn–Wall–Ozawa models based on the multiheating rate method to investigate the degradation kinetics of various rubber composites [10–18].

The basically existing multiwalled halloysite nanotubes (HNT), which are uniformly strong, have a composition similar to montmorillonite and a shape similar to CNT. They are comprised of silicon, aluminum, oxygen, and hydrogen and have a tubular architecture. They have a high aspect ratio and specific surface area, as well as lower surface energy and less filler aggregation [19]. The mechanical, ageing, and gas barrier properties of rubber-HNT nanocomposites [20–26] have been studied extensively in the literature. However, there are just a few exact studies showing the effect of HNT on rubber nanocomposites' thermal behavior. In SBR nanocomposites supplemented with HNT, Rybinski et al. [27] found that the rate of heat breakdown was reduced. The effect of activated HNT and modified HNT in lowering the rate of thermal breakdown and flammability in SBR and ACM [28, 29] was also shown by the same authors.

Carbon black (CB) is a typical filler that is utilized in large quantities (>30 phr) to determine the best qualities in elastomeric goods. Despite this, carbon black particles have a proclivity for aggregation due to uneven distribution during processing. As a result, the elastomeric sector will mark a watershed moment when enormous quantities of carbon black are replaced with other reinforcements in smaller volumes. The use of black filler is significantly reduced, which reduces the weight of the compound and improves its endurance [30]. Furthermore, it is widely acknowledged that combining two or more reinforcements leads to a significant improvement in the properties of elastomeric composites. As a result, elastomeric composites comprising ordinary black filler hybridized with nano-sized reinforcements (CNT, graphene nanoclay) have gained widespread acceptance among academics and megacorporations.

Several recent research studies in the literature have demonstrated the synergy of CB and nanoreinforcements on the thermal behavior of rubber composites. Natural rubber (NR)/styrene butadiene rubber (SBR) blends (80 : 20) reinforced with CB and CNT hybrid fillers showed enhanced stability, according to Boonmahitthisud and Song [31]. Tagelsir et al. [32] showed that increased CB-CNT interactions improve flouroelastometer's thermal stability. The synergy of CB and nanoclay hybrid fillers on the improved thermal degradation characteristics of butyl rubber tyre curing bladder compounds was demonstrated by Razzaghi-Kashani and Samadi [33]. Natural rubber-CB-graphene hybrid nanocomposites with superior heat stability and viscoelastic properties were created by Zang et al. [34].

Nonetheless, there are few investigations on the thermal behavior of rubber nanocomposites reinforced with the HNT-CB dual-filler system. Improved thermal degradation characteristics in natural rubber nanocomposites supplemented with CB and HNT hybrid fillers were discovered by Ismail et al. [35]. The enhanced thermal properties of nitrile rubber [NBR] and polyvinyl chloride/nitrile hybrid nanocomposites [NBR/PVC] have been attributed by the authors to the synergy between the twin fillers and their enhanced interactions [36, 37].

Acrylic Rubber (ACM) is a well-known synthetic elastomer that is utilized in applications requiring high fuel resistance and thermo-oxidative resistance. It is mostly utilized in the automobile industry to make seals, o-rings, and gaskets. Slusarski et al. [38] investigated the thermal behavior of acrylic rubber utilized as sealing plate components. However, there is a scarcity of research in the literature that characterizes the thermal stability of acrylic rubber. To the best of the author's knowledge, there are no previous studies on the thermal stability, degradation kinetics, or dynamic mechanical characteristics of ACM composites reinforced with HNT-CB hybrid filler systems. The thermal properties of ACM composites (filled simply with 70 phr CB) and ACM hybrid composites comprising a fixed amount of CB (60 phr) and a variable amount of halloysite nanotubes (HNT) (2, 4, 6, 8, and 10 phr) were investigated in this study, which builds on prior research [39]. In this research work, thermo-oxidative stability, thermal decomposition kinetics, and temperature of glass transition were explored using oxidation induction time, thermogravimetric, and dynamic mechanical investigations, respectively, to evaluate the thermal characteristics.

2. Experiment

2.1. Materials. RK Polymers, Chennai, India, provided the elastomeric matrix Acrylic Rubber, AR801 (45 Mooney units). Sigma Aldrich in Germany provided the halloysite nanotubes (50 nm). BP Chemicals, Pune, India, provided the carbon black (FEF N550), antioxidant (Naugard 445), plasticizer (DOP), processing aid (Rubaid 2220), cure

(sulphur MC), accelerators (potassium stearate, sodium stearate), and other compounding elements indicated in Table 1. All the compounding ingredients used were of commercial grade.

2.2. Preparation of ACM Composites. Table 1 shows the ACM composite formulas. A dual-roll mill with dimensions of 160 mm × 320 mm was used to compound the material. The two-roll mill was operated at atmospheric temperature, and the speed ratio of the rotors was maintained at 1 : 14. The blending sequence began with the introduction of ACM rubber into the mill. HNT was subsequently included after a few minutes of mastication, and the mixing was continued for 10 minutes. The antioxidant, activator (stearic acid), CB, and plasticizer were then added to the mix, which was mixed for another 20 minutes. Sulphur, potassium stearate, and sodium stearate were added last and mixed for another 2-3 minutes. It was possible to create a homogeneous compound. With atomic weights of 0, 2, 4, 6, 8, and 10% for HNT, six distinct compounds were created. These compounds are first cured in an electric press at 160°C before being postcured in a 150°C oven for 4 hours. These vulcanizates were treated for various characterisations after being kept in an ambient environment for 24 hours.

3. Characterisation

3.1. Stability of Oxidation. Oxidation induction time is used to determine the thermo-oxidative stability of the composites (OIT). OIT measurements are performed using an ISO 11357-compliant differential scanning calorimeter (DSC 6000, SII NANO Technology, Japan). The specimens are heated to 200°C in a nitrogen environment at a rate of 20°C/min. The specimens are kept at that temperature for 5 minutes to reach equilibrium before being introduced to oxygen. The commencement of oxidation in the sample is indicated by a significant increase in heat flow. The time difference between the start of oxidation and the first contact with oxygen is used to compute the sample's OIT.

3.2. Thermogravimetric Analysis. Under nitrogen atmosphere, the thermal degradation behavior of ACM composites was investigated using a thermogravimetric analyser (TG/DTA 6200, SII NANO technology, Japan). Samples weighing 7-8 mg were heated at 2.5, 5, 10, and 15°C/min under nitrogen from 30°C to 600°C.

3.3. Determination of Energy of Activation Energy (E_a). To investigate the thermal behavior of any polymeric substance, it is critical to quantify its thermal degradation kinetics, which is commonly described using the Arrhenius equation (40).

$$k = A \exp \frac{(-E_a)}{RT}, \tag{1}$$

where E_a represents energy of activation (kJ/mol), A is a representation of the preexponential factor, T denotes the absolute temperature (K), and R connotes gas constant.

The following equation can be used to calculate the rate of reaction [40]:

$$\frac{d\alpha}{dt} = k\, f(\alpha). \tag{2}$$

Here, t (s) denotes the time of reaction, f indicates a function related to the reaction mechanism, K represents the rate constant, and α signifies the conversion degree which is expressed as [40]

$$\alpha = \frac{(m_0 m_t)}{(m_0 - m_f)}, \tag{3}$$

where m_o, m_i, and m_f, respectively, denotes rubber composites' initial, final, and actual weights as determined from the thermogravimetric curves.

Combining equations (1) and (2) the following equation is obtained:

$$\frac{d\alpha}{dt} = f(\alpha) \exp \frac{(-E_a)}{RT}. \tag{4}$$

The apparent activation energy for nonisothermal degradation (E_a) could be determined using the differential Kissinger or integral Flynn–Wall–Ozawa techniques. The Kissinger method, or alternatively called the peak-maximum evolution method, uses the point where the rate of reaction during heating is at its maximum (Tp) to calculate the activation energy. Furthermore, the Kissinger approach yields only a single activation energy value for the entire decomposition process. The Kissinger approach calculates the kinetic parameters that are independent of the conversion.

On the other hand, the Flynn–Wall–Ozawa approach calculates the activation energy based on the temperature that corresponds to a certain conversion degree (Ta), the so called isoconversional method. This allows to calculate the apparent activation energy as a function of the conversion degree. This method also provides information on the conversion levels at which more energy is required to break the main bonds of the polymeric chain during the thermal degradation process.

3.3.1. Kissinger Differential Method. The differential method endorses the following expression [41]:

$$\ln\left(\frac{\beta}{T_{\max}^2}\right) = \ln\left(\frac{AR}{g(\alpha)E_a}\right) - \frac{E_a}{RT_{\max}}, \tag{5}$$

where β indicates rate of heating (K/min), $T_{\max}$ represents the peak temperature as determined from DTG curve α connotes samples' mass conversion degree, and A indicates the factor preexponential R denotes the ideal gas constant. E_a symbolises activation energy.

Graphs drawn using $\ln(\beta/T^2_{\max})$ against $(1/T_{\max})$ resulted in a fitted straight line, and the slope of the straight line $(-E_a/R)$ can be used to determine the energy of activation E_a.

Table 1: ACM hybrid nanocomposites formulation table.

Ingredients (Phr[a])	Compounds					
	CB70	CB60-HNT2	CB60-HNT4	CB60-HNT6	CB60-HNT8	CB60-HNT10
ACM	100	100	100	100	100	100
HNT	0	2	4	6	8	10
Stearic acid	1.5	1.5	1.5	1.5	1.5	1.5
Naugard 445[b]	2	2	2	2	2	2
FEF N550	70	60	60	60	60	60
Rubaid222[c]	2	2	2	2	2	2
DOP[d]	5	5	5	5	5	5
Sulphur MC	0.3	0.3	0.3	0.3	0.3	0.3
Sodium stearate	3	3	3	3	3	3
Potassium stearate	0.3	0.3	0.3	0.3	0.3	0.3

[a]Parts by weight per hundreds of rubbers, [b]4-4′-bis (*α*-*α*-dimethyl benzyl) diphenyl amine, [c]pentaerythritol stearate, and [d]dioctyl phthalate.

3.3.2. Flynn–Wall–Ozawa Integral Method. The integral method acknowledges the following expression [42–44]:

$$\log\beta = \log\left(\frac{AE_a}{R\,g(\alpha)}\right) - 2.315 - 0.4567\frac{E_a}{RT}. \quad (6)$$

At a given conversion degree α, graphs drawn using $\log\beta$ versus $1/T$ generates a straight line having $0.457 \times -E_a/R$ as slope. The slope thus obtained is used to determine the activation energy (E_a).

3.4. Dynamic Mechanical Analysis (DMA). The composites' thermomechanical behavior was assessed. Using a DMA analyser, the storage modulus (E) and loss tangent were measured against temperature (6100, SII NANO Technology, Japan). In tension mode, these properties were determined at a frequency of 1 Hz and a strain of 0.2 percent. The temperature sweep trials were carried out at a rate of $5^{\circ}\mathrm{C\,min^{-1}}$ between −100°C and 100°C.

4. Discussion of the Findings

4.1. Short-Term Oxidation. OIT is commonly used to verify antioxidative performance; a higher OIT value indicates that the sample is more resistant to thermal oxidation. Table 2 lists the OIT values for ACM composites generated from DSC measurements (as shown in Figure 1).

ACM composites reinforced with these twin fillers have significantly better short-term oxidation values than carbon black-reinforced ACM composites. Among the numerous composites studied, the ACM composite reinforced with 6 phr had the greatest OIT value. The production of intercalated morphology (HNT-ACM-CB) and homogeneous distribution of tubular nanofiller in the ACM rubber matrix may be ascribed to the notable increase in OIT value of ACM composites [28]. These variables increase the likelihood of contact between the rubber and the antioxidants supplied during compounding and prevent the antioxidants from diffusing to the surface of the ACM matrix, even when exposed to heat and oxygen. This increases the antiaging effect by delaying the radical reaction [34]. These remarkable findings clearly show that tubular nanofiller has a major impact on delaying the onset of oxidation in ACM rubber composites.

The OIT value drops with the addition of 8 phr HNT to the rubber matrix, indicating a crucial destructive effect on the thermo-oxidative stability of ACM composites. This could be due to poor filler-matrix compatibility, increased filler-filler interaction, or the production of agglomerates. These conditions limit the interfacial contacts between the rubber and antioxidants, allowing most antioxidants to diffuse to the rubber matrix's surface under heat and oxygen, speeding up the formation of radical reactions and delaying the antiaging effect [45].

4.2. Analysis of Thermogravimetric Data. Figure 2 represents the thermal degradation characteristics of ACM composites at 5°C/min. ACM conventional and hybrid nanocomposites have a single degradation step. The incorporation of HNT nanofiller in CB-filled ACM composites improves the degradation temperature at 10 percent weight loss and at 50 percent weight loss (T_{50}), as shown in Figure 2 and Table 3. Furthermore, the char residue concentration of ACM composites reinforced with CB and HNT is 41.24 percent, 41.42 percent, 42.44 percent, 42.14 percent, and 41.29 percent, indicating that HNT plays an important role in enhancing the thermal degrading behavior of ACM composites.

As can be observed from the peak of the first derivative shown in Figure 3, the temperature at which the rate of degradation ($T_{\max}$) of ACM composites filled with CB is maximum is at its maximum 418°C. ACM composite reinforced with 2 to 10 phr of HNT demonstrated $T_{\max}$ values of 419°C, 422°C, 430°C, 421°C, and 419°C. It is highly evident that, among all the composites investigated, ACM composite reinforced with 6 phr HNT demonstrated the highest $T_{\max}$. The better performance of ACM composites with 6 phr HNT can be attributed to a uniform distribution of tubular nanofiller in the ACM rubber matrix, the development of intercalated morphology, superior crosslink network creation, and significant ACM-CB-HNT interactions, as evident from the highest T_g value of −22.7°C discussed in the viscoelastic studies discussed in the later part. These variables encourage a convoluted path to the ACM breakdown products, preventing the polymer from degrading further. However, it can be noticed that beyond 6 phr of HNT, $T_{\max}$ decreases with further increases in HNT

Table 2: OIT values of ACM composites at 200°C.

Sample	CB70	CB60-HNT2	CB60-HNT4	CB60-HNT6	CB60-HNT8	CB60-HNT10
OIT (min)	89.5	104.43	110.54	113.31	109.51	108.59

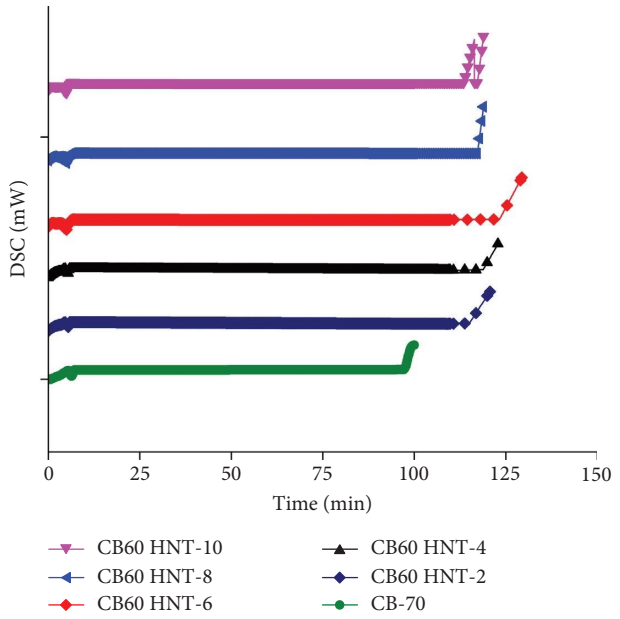

Figure 1: OIT values of ACM composites.

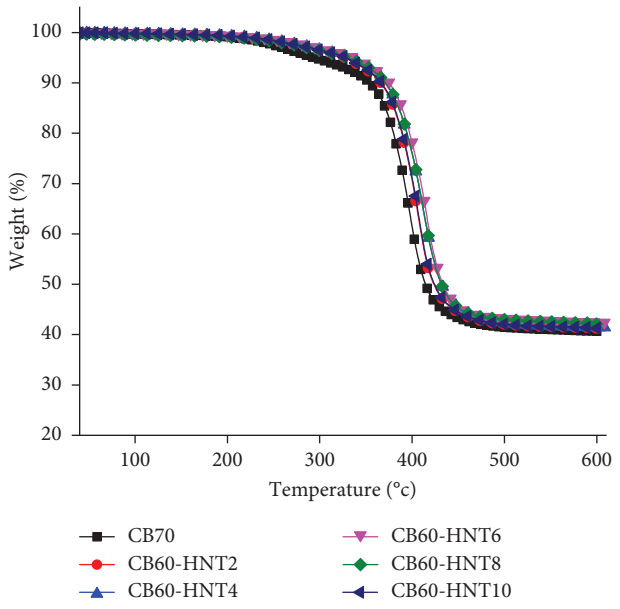

Figure 2: TGA curves of ACM composites at 10°C/min under nitrogen atmosphere.

loading. Such a reduction in T_{max} values can be ascribed to poor compatibility between ACM and HNT, agglomeration of HNT tubules, partial debonding of large agglomerates from the elastomeric matrix, and the subsequent formation of interfacial voids. Butyl rubber nanocomposites [33], NBR-CB-HNT [36], and NBR/PVC-CB-HNT [37] hybrid nanocomposites showed similar findings.

4.3. Analysis of Kinetics. The kinetic parameters must be examined in order to gain a better understanding of the mechanism of ACM degradation and to conduct a comprehensive investigation into the influence of hybrid fillers. Among the several composites studied, ACM-CB60-HNT6 showed higher antiaging and TGA. As a result, non-isothermal assessments at various heating rates were used to investigate the decomposition of conventional composite (ACM-CB70) and ACM-CB60-HNT6 alone in this work. The TGA and DTG curves of ACM-CB70 at various heating rates are depicted in Figures 4 and 5. Figures 6 and 7 show the TGA and DTG curves of ACM-CB60-HNT6 at various heating rates.

4.4. The Kissinger Approach. Figure 8 shows the graph of ln (β/T^2_{max}) against $(1/T_{max})$ for the evaluation of E_a using the differential method. Table 4 shows a summary of the findings. 521 kJ/mol is the activation energy of a CB-filled ACM composite reinforced with CB filler. With the addition of 6 phr HNT content, it is enhanced to 543 kJ/mol, indicating that HNT improves the thermal stability of ACM composites. The increased HNT-ACM-CB interactions and the homogeneous distribution of tubular nanofiller in the ACM matrix have resulted in such a dramatic improvement.

4.5. Flynn–Wall–Ozawa Method. The integral method is used to determine the E_a for a given degree of conversion (α) using graphs of log versus $1/T$. The Flynn–Wall–Ozawa pattern of ACM composites reinforced with CB and ACM composites reinforced with CB and 6 phr of HNT is depicted in Figures 9 and 10. The graphs of log against $1/T$ generated for carbon black-filled ACM composite and dual filler reinforced ACM composites yield fitted straight lines with high linearly correlation coefficient for varied values of α. It should also be mentioned that these straight lines, which were achieved for a variety α are for the composites under consideration, which are almost parallel to one another, and all of the correlation coefficients are around 0.95, indicating that the approach is highly acceptable to ACM composites.

The plot of activation energy (E_a) as a function of α are presented in Figure 11. On the basis of the trend of E_a, by which both composites achieve values that show the oxidative cross-linking process that occurs during the heat deterioration of acrylic rubber [46], it may be deduced that the levels of activation energy (E_a) acquired using the Flynn–Wall–Ozawa approach are slightly higher in comparison to the value obtained using the Kissinger approach [10–18]. Furthermore, these figures demonstrate the significance of HNT in enhancing the thermal stability of the ACM matrix. When the ACM hybrid composites were heated to disintegrate, the local (HNT-CB) hybrid filler network in the rubber formed protective layers over time to protect the underlying rubber matrix. As a result, the pace at

Table 3: TGA characteristics of ACM composites.

Sample	Temperature at 10% weight loss T_{10} (°C)	Temperature at 50% weight loss T_{50} (°C)	Maximum temperature of degradation T_{max} (°C)	Char residue weight (%) at 600 (°C)
CB70	355	415	418	40.68
CB60-HNT2	365	424	419	41.24
CB60-HNT4	367	431	422	41.42
CB60-HNT6	380	434	430	42.44
CB60-HNT8	371	431	421	42.14
CB60-HNT10	366	424	419	41.29

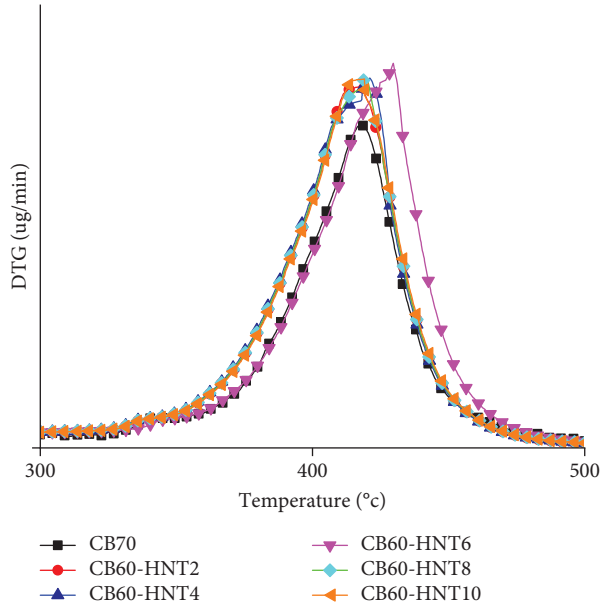

Figure 3: DTG curves of ACM composites at 10°C/min under nitrogen atmosphere.

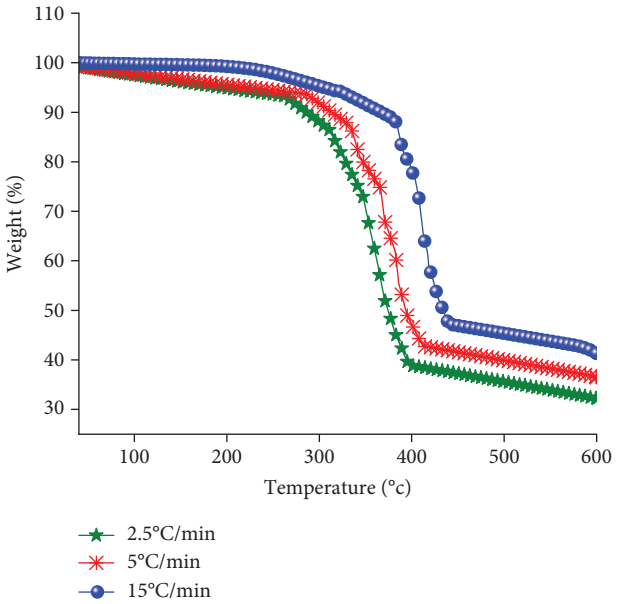

Figure 4: TGA curves of ACM-CB70 composites at different heating rates under nitrogen atmosphere.

which degradation products diffuse has slowed. As a result, the ACM rubber is protected from further deterioration, resulting in an increase in E_a [40]. Clay and carbon black-reinforced hydrogenated nitrile rubber have shown similar results [40].

4.6. ACM Composites' Viscoelastic Behavior

4.6.1. 1 The Influence of Temperature on Storage Modulus. The storage modulus of a composite is a measure of its stiffness. Figure 12 and Table 5 show the storage modulus (E') of the various ACM composites investigated.

It is worth noting that the addition of HNT filler to the ACM matrix results in a significant increase in E'. When compared to a CB-filled ACM composite, all ACM hybrid nanocomposites are always shown to have E' values that are higher at all temperatures. In comparison to CB-filled ACM composites at the same temperature, the storage modulus of ACM hybrid nanocomposites containing 2, 4, 6, 8, and 10 phr of HNT increased by 41 percent, 69 percent, 79 percent, 54 percent, and 50 percent, respectively, at 30°C. Higher cross-link creation can be attributed to the superior performance of ACM composites reinforced with both HNT and CB, and it is also a strong indication of HNT's reinforcing function. Increases in HNT content beyond 6 phr invariably result in poor

HNT dispersion, poor compatibility between the filler and matrix, increased filler-filler interaction, and the eventual development of agglomerates. As a result, the free volume of the matrix enclosing these agglomerates is increased, resulting in increased polymer chain flexibility and a decrease in the storage modulus of the ACM composites [47].

4.6.2. The Influence of Temperature on the Loss Factor. Dynamic mechanical analysis is also used to assess the effect of fillers on the mobility of adjacent elastomeric chains. During the glass transition, a large amount of energy is dissipated due to the viscous movement of long-range polymer chains. The peak height of the damping term loss factor depicts the mobility of the polymer segments (tanδ). Any decrease in the peak height of the loss factor indicates that the mobility of polymer segments is restricted. In elastomeric composites, such a restriction correlates to an

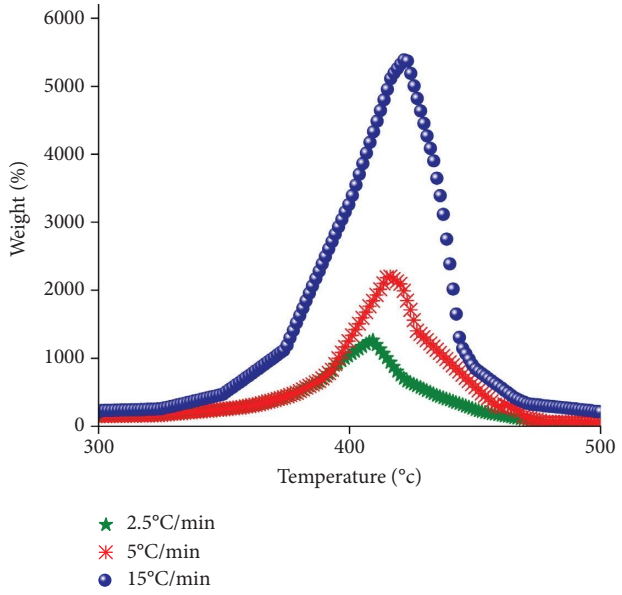

Figure 5: DTG curves of ACM-CB70 composites at different heating rates under nitrogen atmosphere.

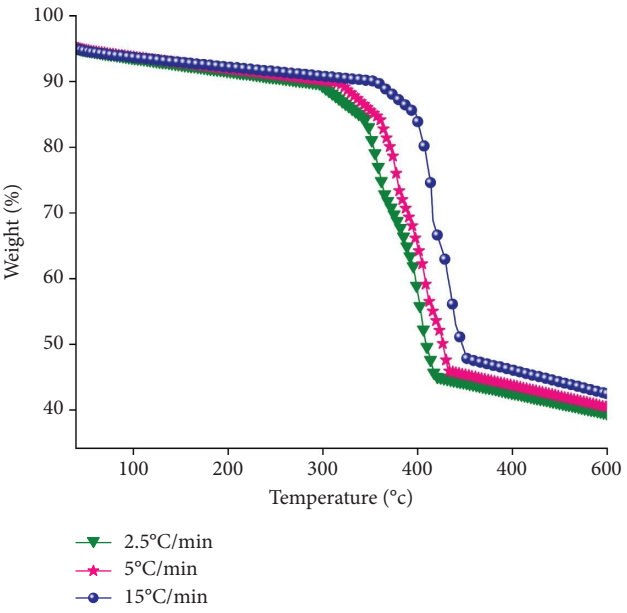

Figure 6: TGA curves of ACM-CB60-HNT6 composites at different heating rates under nitrogen atmosphere.

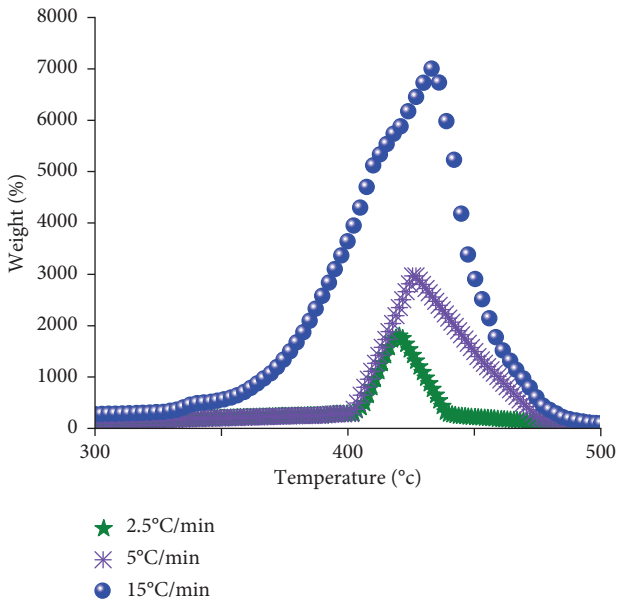

Figure 7: DTG curves of ACM-CB60-HNT6 composites at different heating rates under nitrogen atmosphere.

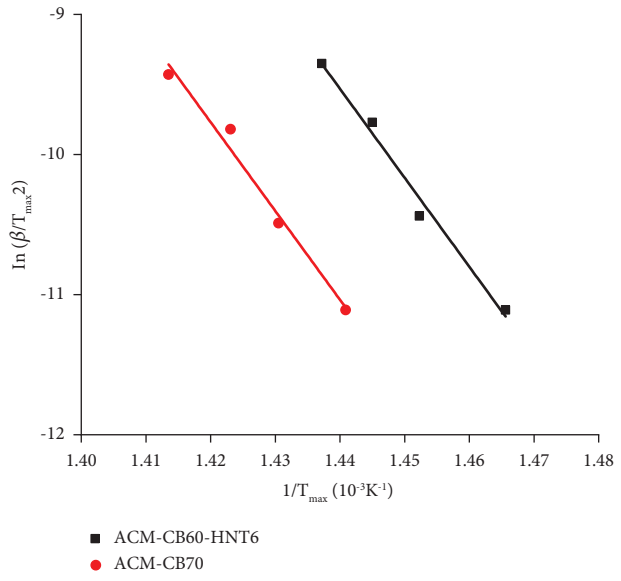

Figure 8: Kissinger plot applied to TGA data of ACM composites at different heating rates.

increase in interfacial adhesion. As compared to composites reinforced with black filler alone, all hybrid composites had lower peak heights, as shown in Figure 13. Furthermore, ACM composites reinforced with 6 phr HNT content had the lowest peak height, indicating that a large proportion of ACM chains were restricted in their mobility. The temperature that corresponds to the highest point, tanδ, shows the glass transition (T_g). It can be seen in Figure 12 that an ACM composite filled with a single filler (CB) has a T_g value of −25.2°C. In ACM composites reinforced with twin fillers, there is also a noticeable movement in T_g values towards higher values.

Table 4: Activation energy (E_a) calculated following the Kissinger method.

Sample	E_a (kJ/mol)	R^2
ACM-CB70	521	0.984
ACM-CB60-HNT6	543	0.981

Furthermore, ACM composites containing 6 phr HNT loading had the highest T_g value of −22.7°C of all the composites studied. The motility of ACM chains in the vicinity of the twin filler network was reduced by a homogeneous distribution of black filler and tubular HNT in

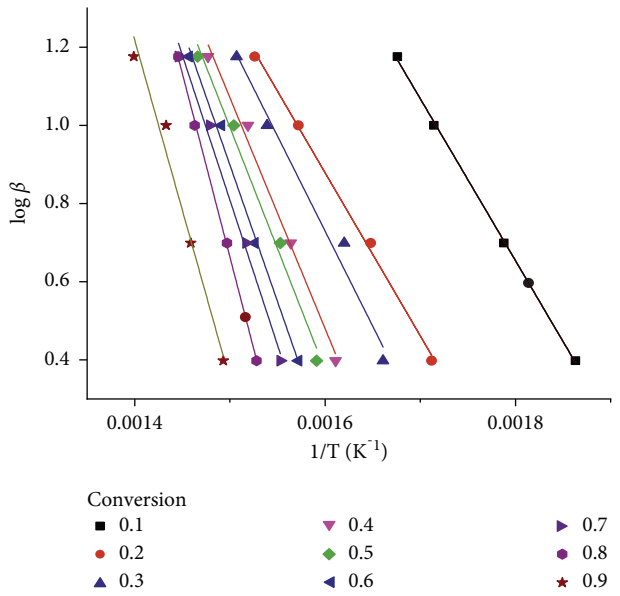

Figure 9: Flynn–Wall–Ozawa plot of ACM-CB70 conventional composites.

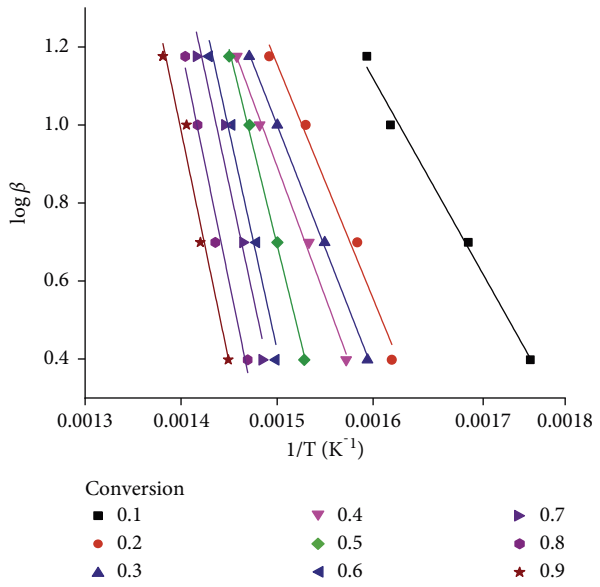

Figure 10: Flynn–Wall–Ozawa plot of ACM-CB60-HNT6 hybrid nanocomposites.

the ACM matrix, as well as increased HNT-ACM-CB interfacial contacts. As a result, the T_g value of all ACM composites reinforced with hybrid reinforcement is shifting towards higher values. It was also discovered that ACM composites with 8 phr and 10 phr of HNT content had lower T_g values than ACM composites with 6 phr HNT reinforcement. Agglomerates are formed when the nanotubular filler content exceeds 6 phr. As a result, the free volume of the matrix enclosing these agglomerates is increased, resulting in easy chain motion and a reduction in the T_g of the ACM composites [48]. NBR-CB-HNT [36] and natural rubber-CB-nanoclay [49] hybrid nanocomposites showed similar results.

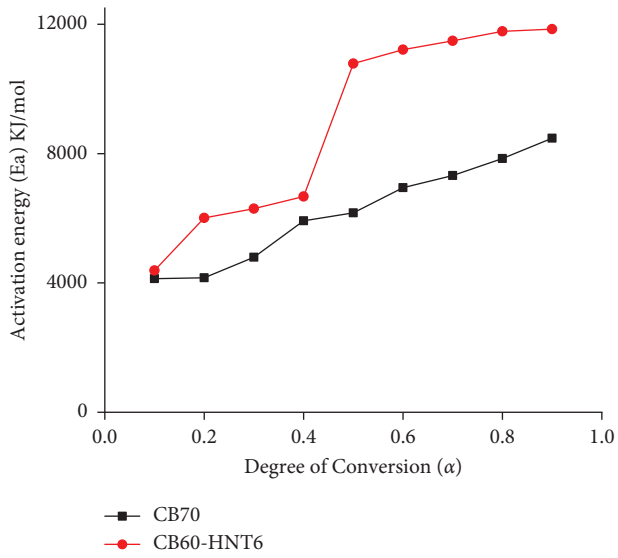

Figure 11: Activation esnergy vs. conversion degree (α).

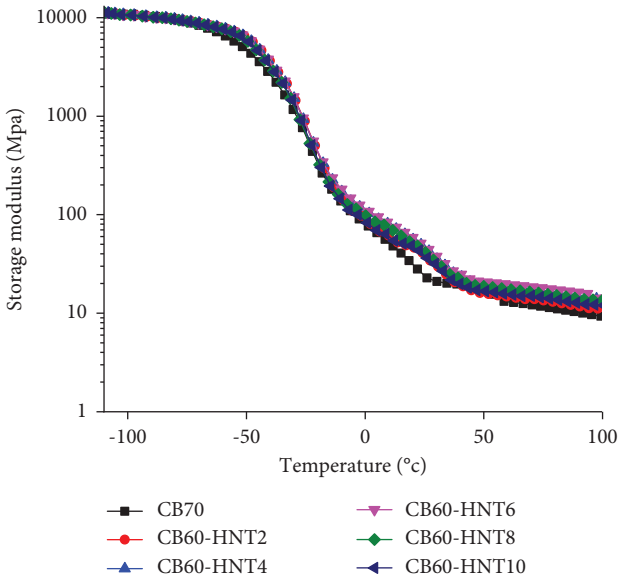

Figure 12: Variation of storage modulus (E') with temperature for ACM composites.

Table 5: Dynamic mechanical properties of ACM composites.

Samples	Storage modulus (MPa) at different temperatures (°C)						T_g (°C)
	−70	−50	−30	30	50	70	
CB70	8348.93	5062.64	1167.07	21.03	15.67	12.13	−25.2
CB60-HNT2	8759.21	6513.60	1441.01	29.62	16.69	13.96	−24.2
CB60-HNT4	8844.47	6599.03	1526.44	35.41	19.02	16.80	−23.9
CB60-HNT6	8891.72	6638.60	1566.01	37.62	20.68	18.46	−22.7
CB60-HNT8	8834.17	5742.79	1516.01	32.40	18.69	16.46	−23.1
CB60-HNT10	8774.26	6050.39	1456.03	31.62	16.69	14.96	−24.8

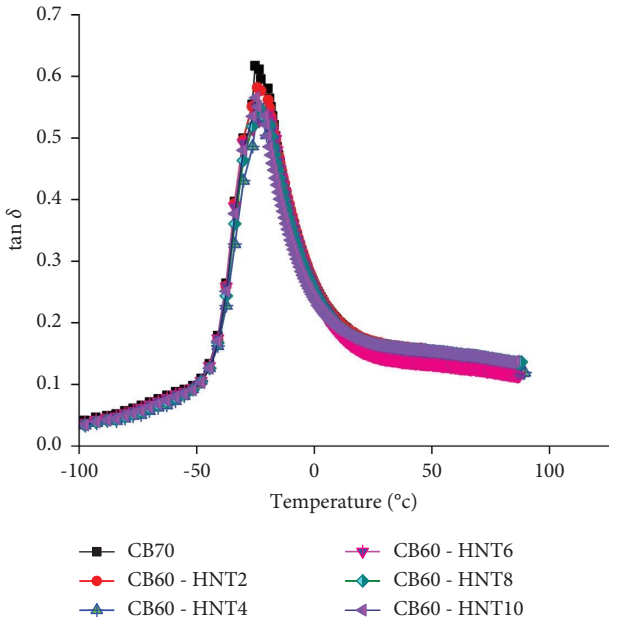

Figure 13: Deviation of loss factor (tanδ) vs. temperature.

5. Conclusion

The effect of HNT filler on the thermal properties of black filler-reinforced ACM composites was investigated in this study. When compared to a standard composite, composites containing twin fillers displayed excellent thermal breakdown properties and outstanding anti-oxidation performance. Furthermore, the use of differential and integral approaches to assess thermal degradation kinetic parameters revealed an increase in the activation energy of ACM composites when a tubular nanofiller was added. The storage modulus was increased by 79 percent at 30°C when 10 phr of black filler was replaced with 6 phr of tubular HNT, according to dynamic mechanical analysis. This work is expected to pave the way for the use of HNT as reinforcement in ACM rubber, and it also has great potential for rubber seal manufacturers.

Data Availability

All the data are presented within the manuscript.

Conflicts of Interest

The authors declare that they have no conflicts of interest.

Authors' Contributions

All authors discussed the content of the article based on their domain expertise on the subjects presented. K. Senthilvel framed and performed the experiments. B. Prabu and C. Moganapriya performed characterization studies like DMA and TGA. M. Francis Luther King assisted in analyzing the results. R. Rajasekar and Md. Elias Uddin supervised the study, discussed the results, proofread the manuscript, and confirmed its findings.

Acknowledgments

The authors would like to express their gratitude to Tech Centre, Ramcharan Chemicals, Chennai, and KELVN Labs, Hyderabad, for assisting them with sample preparation and testing.

References

[1] G. Janowska, A. Kucharska-Jastrząbek, and P. Rybiński, "Thermal stability, flammability and fire hazard of butadiene-acrylonitrile rubber nanocomposites," *Journal of Thermal Analysis and Calorimetry*, vol. 103, no. 3, pp. 1039–1046, 2011.

[2] G. Sui, W. H. Zhong, X. P. Yang, Y. H. Yu, and S. H. Zhao, "Preparation and properties of natural rubber composites reinforced with pretreated carbon nanotubes," *Polymers for Advanced Technologies*, vol. 19, no. 11, pp. 1543–1549, 2008.

[3] P. Rybiński, R. Anyszka, M. Imiela, M. Sicinski, and T. Gozdek, "Effect of modified graphene and carbon nanotubes on the thermal properties and flammability of elastomeric materials," *Journal of Thermal Analysis and Calorimetry*, vol. 127, no. 3, pp. 2383–2396, 2017.

[4] A. Krainoi, C. Kummerloewe, Y. Nakaramontri et al., "Influence of carbon nanotube and ionic liquid on properties of natural rubber nanocomposites," *Express Polymer Letters*, vol. 13, no. 4, pp. 327–348, 2019.

[5] J. Heidarian, A. Hassan, and N. M. M. A. Rahman, "Improving the thermal properties of fluoroelastomer (Viton GF-600S) using acidic surface modified carbon nanotube," *Polímeros*.vol. 25, no. 4, pp. 392–401, 2015.

[6] Y. Wang, X. Qiu, and J. Zheng, "Effect of the sheet size on the thermal stability of silicone rubber–reduced graphene oxide nanocomposites," *Journal of Applied Polymer Science*, vol. 136, no. 5, pp. 47034–47042, 2019.

[7] B. Chen, N. Ma, X. Bai, H. Zhang, and Y. Zhang, "Effects of graphene oxide on surface energy, mechanical, damping and thermal properties of ethylene-propylene-diene rubber/petroleum resin blends," *RSC Advances*, vol. 2, no. 11, pp. 4683–4689, 2012.

[8] J. W. Gilman, C. L. Jackson, A. B. Morgan et al., "Flammability properties of polymer– layered-silicate nanocomposites. Polypropylene and polystyrene nanocomposites," *Chemistry of Materials*, vol. 12, no. 7, pp. 1866–1873, 2000.

[9] S. Vyazovkin, I. Dranca, X. Fan, and R. Advincula, "Kinetics of the thermal and thermo-oxidative degradation of a polystyrene–clay nanocomposite," *Macromolecular Rapid Communications*, vol. 25, no. 3, pp. 498–503, 2004.

[10] W. Ahn and H. S. Lee, "Non-isothermal TGA study on thermal degradation kinetics of ACM rubber composites," *Elastomers and Composites*, vol. 48, no. 2, pp. 161–166, 2013.

[11] A. Choudhury, A. K. Bhowmick, C. Ong, and M. Soddemann, "Effect of various nanofillers on thermal stability and degradation kinetics of polymer nanocomposites," *Journal of Nanoscience and Nanotechnology*, vol. 10, no. 8, pp. 5056–5071, 2010.

[12] S. P. Ammineni, C. Nagaraju, and D. Lingaraju, "Thermal degradation of naturally aged NBR with time and temperature," *Materials Research Express*, vol. 9, no. 6, Article ID 065305, 2022.

[13] J. Zhang, J. Li, M. Liu, Y. Zhao, and S. Wang, "Thermal decomposition kinetics and mechanism of low-temperature hydrogenated acrylonitrile butadiene rubber composites with sodium methacrylate," *Chemical Research in Chinese Universities*, vol. 32, no. 6, pp. 1045–1051, 2016.

[14] S. Krishnamurthy and P. Balakrishnan, "Dynamic mechanical behavior, solvent resistance and thermal degradation of nitrile rubber composites with carbon black-halloysite nanotube hybrid fillers," *Polymer Composites*, vol. 40, no. S2, pp. 1612–1621, 2019.

[15] X. Xiong, J. Wang, H. Jia, E. Fang, and L. Ding, "Structure, thermal conductivity, and thermal stability of bromobutyl rubber nanocomposites with ionic liquid modified graphene oxide," *Polymer Degradation and Stability*, vol. 98, no. 11, pp. 2208–2214, 2013.

[16] Z. H. Wu, B. Zhou, Q. X. Fan, and Y. J. Cai, "Thermal degradation kinetics investigation on Nano-ZnO/IFR synergetic flame retarded polypropylene/ethylene-propylene-diene monomer composites processed via different fields," *E-Polymers*, vol. 19, no. 1, pp. 50–60, 2019.

[17] J. S. Oh, J. M. Lee, and W. S. Ahn, "Non-isothermal TGA analysis on thermal degradation kinetics of modified-NR rubber composites," *Polym.Korea*, vol. 33, no. 5, pp. 435–440, 2009.

[18] K. Subramaniam, A. Das, L. Häußler, C. Harnisch, K. W. Stöckelhuber, and G. Heinrich, "Enhanced thermal stability of polychloroprene rubber composites with ionic liquid modified MWCNTs," *Polymer Degradation and Stability*, vol. 97, no. 5, pp. 776–785, 2012.

[19] B. Singh, "Why does halloysite roll?—a new model," *Clays and Clay Minerals*, vol. 44, no. 2, pp. 191–196, 1996.

[20] P. Pasbakhsh, H. Ismail, M. A. Fauzi, and A. A. Bakar, "EPDM/modified halloysite nanocomposites," *Applied Clay Science*, vol. 48, no. 3, pp. 405–413, 2010.

[21] S. Rooj, A. Das, V. Thakur, R. Mahaling, A. K. Bhowmick, and G. Heinrich, "Preparation and properties of natural nanocomposites based on natural rubber and naturally occurring halloysite nanotubes," *Materials & Design*, vol. 31, no. 4, pp. 2151–2156, 2010.

[22] H. Ismail, S. Z. Salleh, and Z. Ahmad, "Properties of halloysite nanotubes-filled natural rubber prepared using different mixing methods," *Materials & Design*, vol. 50, pp. 790–797, 2013.

[23] B. Guo, F. Chen, Y. Lei, X. Liu, J. Wan, and D. Jia, "Styrene-butadiene rubber/halloysite nanotubes nanocomposites modified by sorbic acid," *Applied Surface Science*, vol. 255, no. 16, pp. 7329–7336, 2009.

[24] H. Ismail and H. S. Ahmad, "Effect of halloysite nanotubes on curing behavior, mechanical, and microstructural properties of acrylonitrile–butadiene rubber nanocomposites," *Journal of Elastomers and Plastics*, vol. 46, no. 6, pp. 483–498, 2014.

[25] R. Berahman, M. Mehrabi, and S. M. Paran, "Preparation and characterisation of vulcanised silicone rubber/halloysite nanotube composites: effect of matrix hardness and HNT contents," *Materials and Design*, vol. 50, pp. 790–797, 2016.

[26] S. Rooj, A. Das, and G. Heinrich, "Tube-like natural halloysite/fluoroelastomer nanocomposites with simultaneous enhanced mechanical, dynamic mechanical and thermal properties," *European Polymer Journal*, vol. 47, no. 9, pp. 1746–1755, 2011.

[27] P. Rybiński, G. Janowska, M. Jóźwiak, and A. Pajak, "Thermal stability and flammability of butadiene–styrene rubber nanocomposites," *Journal of Thermal Analysis and Calorimetry*, vol. 109, no. 2, pp. 561–571, 2012.

[28] P. Rybiński, G. Janowska, M. Jóźwiak, and M. Jozwiak, "Thermal stability and flammability of styrene–butadiene rubber (SBR) composites," *Journal of Thermal Analysis and Calorimetry*, vol. 113, no. 1, pp. 43–52, 2013.

[29] P. Rybiński, G. Janowska, M. Jóźwiak, and A. Pajak, "Thermal properties and flammability of nanocomposites based on diene rubbers and naturally occurring and activated halloysite nanotubes," *Journal of Thermal Analysis and Calorimetry*, vol. 107, no. 3, pp. 1243–1249, 2012.

[30] S. Kumar, G. B. Nando, S. Nair, G. Unnikrishnan, A. Sreejesh, and S. Chattopadhyay, "Effect of organically modified montmorillonite clay on morphological, physicomechanical, thermal stability, and water vapor transmission rate properties of BIIR-CO rubber nanocomposite," *Rubber Chemistry and Technology*, vol. 88, no. 1, pp. 176–196, 2015.

[31] A. Boonmahitthisud and Z. H. Song, "Effects of carbon black and carbon nanotube on mechanical and thermal properties of 80NR/20SBR composites," *Materials Science Forum*, vol. 654-656, pp. 2783–2786, 2010.

[32] Y. Tagelsir, S. X. Li, X. Lv, S. Wang, S. Wang, and Z. Osman, "Effect of oxidized and fluorinated MWCNTs on mechanical, thermal and tribological properties of fluoroelastomer/carbon black/MWCNT hybrid nanocomposite," *Materials Research Express*, vol. 5, no. 6, Article ID 065318, 2018.

[33] M. Razzaghi-Kashani and A. Samadi, "Physical–mechanical properties of carbon black–nanoclay composites of butyl rubber as curing bladder compounds," *Plastics, Rubber and Composites*, vol. 44, no. 7, pp. 253–258, 2015.

[34] H. Zhang, C. Wang, and Y. Zhang, "Preparation and properties of styrene-butadiene rubber nanocomposites blended with carbon black-graphene hybrid filler," *Journal of Applied Polymer Science*, vol. 132, no. 3, 2015.

[35] H. Ismail, S. Z. Salleh, and Z. Ahmad, "The effect of partial replacement of carbon black (CB) with halloysite nanotubes (HNTs) on the properties of CB/HNT-filled natural rubber nanocomposites," *Journal of Elastomers and Plastics*, vol. 45, no. 5, pp. 445–455, 2013.

[36] K. Senthivel, K. Manikandan, and B. Prabu, "Studies on the mechanical properties of carbon Black/halloysite nanotube hybrid fillers in nitrile rubber nanocomposites," *Materials Today Proceedings*, vol. 2, no. 4-5, pp. 3627–3637, 2015.

[37] K. Senthilvel and B. Prabu, "Novel carbon black-halloysite nanotube reinforced NBR-PVC hybrid oil seals for automotive applications," *Recent Patents on Materials Science*, vol. 11, no. 2, pp. 83–90, 2019.

[38] L. Ślusarski, G. Janowska, and P. Schulz, "Thermal stability and combustibility of rubbers and sealing plates," *Journal of Thermal Analysis and Calorimetry*, vol. 111, no. 2, pp. 1577–1583, 2013.

[39] K. Senthilvel, N. Rathinam, B. Prabu, and A. A. Jeya Kumar, "Investigation on the mechanical and ageing properties of acrylic rubber reinforced halloysite nanotubes/carbon black hybrid composites," *Journal of Elastomers and Plastics*, vol. 53, Article ID 0095244320961826, 2020.

[40] S. Chen, H. Yu, W. Ren, and Y. Zhang, "Thermal degradation behavior of hydrogenated nitrile-butadiene rubber (HNBR)/clay nanocomposite and HNBR/clay/carbon nanotubes nanocomposites," *Thermochimica Acta*, vol. 491, no. 1-2, pp. 103–108, 2009.

[41] H. E. Kissinger, "Reaction kinetics in differential thermal analysis," *Analytical Chemistry*, vol. 29, no. 11, pp. 1702–1706, 1957.

[42] J. H. Flynn and L. A. Wall, "General treatment of the thermogravimetry of polymers," *Journal of Research of the National Bureau of Standards Section A: Physics and Chemistry*, vol. 70A, no. 6, pp. 487–523, 1966.

[43] T. Ozawa, "A new method of analyzing thermogravimetric data," *Bulletin of the Chemical Society of Japan*, vol. 38, no. 11, pp. 1881–1886, 1965.

[44] T. Ozawa, "Thermal analysis-review and prospect," *Thermochimica Acta*, vol. 355, no. 1-2, pp. 35–42, 2000.

[45] J. Lin, Y. Luo, B. Zhong, D. Hu, Z. Jia, and D. Jia, "Enhanced interfacial interaction and antioxidative behavior of novel halloysite nanotubes/silica hybrid supported antioxidant in styrene-butadiene rubber," *Applied Surface Science*, vol. 441, pp. 798–806, 2018.

[46] P. R. Morrell, M. Patel, and A. R. Skinner, "Accelerated thermal ageing studies on nitrile rubber O-rings," *Polymer Testing*, vol. 22, no. 6, pp. 651–656, 2003.

[47] P. Mohanty, T. K. Bastia, D. Behera, and S Panda, "Chitosan grafted carbon nanotubes ReinforcedVinyl ester/UPE blend based partially bio-nanocomposite," *Asian Journal of Chemistry*, vol. 31, no. 9, pp. 1943–1948, 2019.

[48] M. Kalaee, S. Akhlaghi, S. Mazinani, A. Sharif, Y. C. Jarestani, and M. Mortezaei, "Effect of ZnO nanoparticles on kinetics of thermal degradation and final properties of ethylene-propylene-diene rubber systems," *Journal of Thermal Analysis and Calorimetry*, vol. 110, no. 3, pp. 1407–1414, 2012.

[49] Y. Liu, L. Li, and Q. Wang, "Effect of carbon black/nanoclay hybrid filler on the dynamic properties of natural rubber vulcanizates," *Journal of Applied Polymer Science*, vol. 118, no. 2, pp. 1111–1120, 2010.